Concise Rationalised Presentation of **Optimal Wind Turbine Theory**

Distilled from Glauert's pioneering work and the author's papers

Preface:

Existing wind turbine theory is a mess. Glauert's first pass was an aside to his disjointed collection of early propeller theories and missed a simple analytic solution and extension . He was killed by a car before his manuscript was finalised. In the 1960's oil 'crisis' triggered a rush to build big windmills and to encode his windmill offshoot theory and add effects when the basics were still not clearly understood with, and the results became uninterpretable and untrustworthy. Beyond all their complicated empirical corrections there is precious little insight and physical explanation in misnamed wind 'energy' texts. (Oil is a finite energy we squander; wind is a sustainable power flow)

This treatise is a humble attempt to develop stream turbine actuator disc theories systematically and logically with as much generality as possible. It was by retaining generality and using modern vector representations the simple indeed trivial analytic optimal solutions were discovered that had been missed for 70 years and are much easier to present to students. Every attempt is made to explain the meaning and physical significance of analytical and failing those computed results. An emphasis is put on optimisation which is incidentally one of the most revealing tests of a numerical model, yet often hardly mentioned in contemporary wind energy texts which are little more than computer handbooks and most unsuitable as introductory textbooks for anyone new to windpower. This book should be suitable for students who have at least one course in fluid mechanics that includes integral methods and basic aerodynamics and are familiar with vectors and univariate calculus.

The purpose is to give a good starting point in blade and machine design and above all to give a solid clean clear understanding of the basic flow through simple but powerful analysis.

TABLE of CONTENTS

Chapter 1. **Momentum Integral Models**

The actuator disc mean approximation

Full numerical solution of wind turbine flow by CFD or even vortex computations is still today a daunting computer task, principally due to the interaction of the discrete blades and the wake. Propellers were highly developed by the 1930's by combining simple vortex results , momentum and energy integral balances, airfoil blade theory and a basic actuator vortex disc representation . The same methods can be judiciously used for many insights into optimal wind turbines especially the dominant horizontal axis (Hawt) type.....

The full vortex picture is easy enough to sketch for a Hawt. There are vortex loops from the bound vorticity in the blades that are released into the wake at the apparent wind angle greatest at the tip and none at the root. In the actuator approximation of steady axisymmetric flow from an infinity of blades, components can be assembled from all the blade vortices to form paired concentric tubes of axial vortex lines and circumferential vortex rings emanating from an actuator disc of bound vorticity. If the pair move the same axial distance in a revolution, then their axial vorticity components are equal and opposite. If the blades have constant circulation there is just a root axial vortex and a tip tube of axial vorticity and vortex rings.

The approximation effectively time averages the flow through the rotor swept area in a steady stream, averaging out the passage of the blades and the gaps between them as if the net effect was a semi-permeable 'actuator' screen of the bound vorticity that slows the though flow. In practice it has only proved necessary to correct for the finite number of blades at their tips.

Basic equations at wind axis actuator disc.

Just in front of an actuator disk rotating at angular velocity Ω, irrotationality requires the angular velocity induced by any axisymmetric shape of trailing vortex wake to exactly cancel that induced by the bound vorticity of the actuator disc. Since this bound vortex sheet induces equally and oppositely on its two sides, if the (average) angular velocity increase across the disc is ω, the angular velocity induced by the wake alone on the disc must be $\frac{1}{2}\omega$ [1].

The ω increase is reacting to the torque Γ exerted by the flow on the blades: $d\Gamma = r^2 \omega \rho dQ$ (1) where ρ is the fluid density and the infinitesimal volume flux is $dQ = u dS$, u the axial velocity at the rotor, and dS the annular area at radius r. The drop in flow total energy $\Delta H dQ = dP = \Omega d\Gamma$ is the power removed, so $\Delta H = \rho \Omega \omega r^2$ (2)

Since swirl kinetic energy is added across the disc, the pressure drop is $\Delta p = \rho(\Omega + \frac{1}{2}\omega)\omega r^2$ (3)

Wake Model

If a wake annulus expands **ideally** from radius r to r_1 (Figure 1) the axial velocity drops to u_1 such that $u_1 dr_1^2 = u dr^2 = dQ/\pi$ to conserve mass and ω drops to ω_1 with $\omega_1 r_1^2 = \omega r^2$ to conserve

angular momentum and to regain some pressure. Then the head is both H-ΔH and
$H_1 = p_1 + 1/2\rho(u_1^2 + \omega_1^2 r_1^2)$ and $\omega_1^2 r_1^2 = (\omega r^2/r_1^2)^2 r_1^2 = (\omega r)^2 r^2/r_1^2$ (4)

Consider the inevitable real fluid viscous decay of this wake. Ultimately in the 'far' wake, the axial velocity deficit V-u_0 will spread into the wind, dissipating the associated kinetic energy at a further additional loss to the **wind** beyond the extracted power, as explicitly demonstrated by Corten [9].

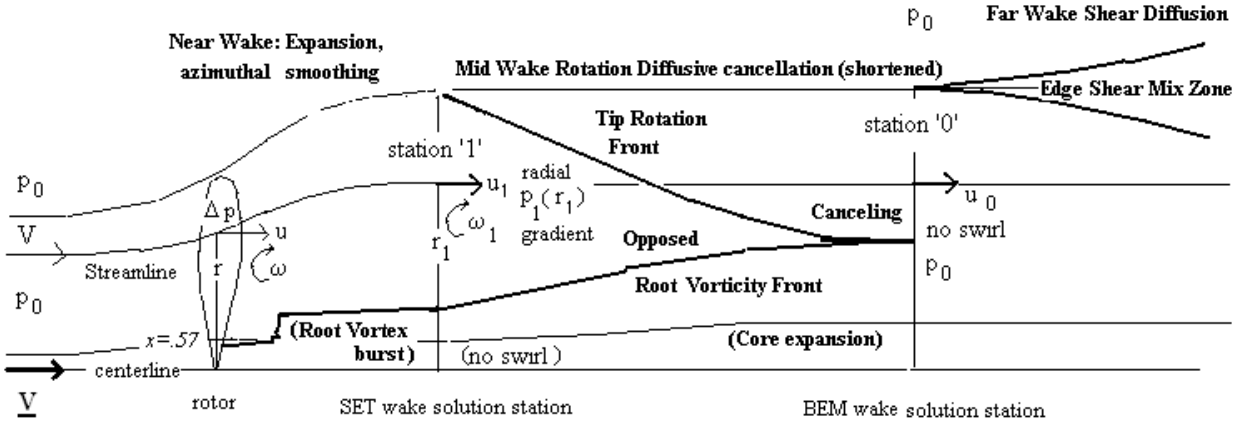

Fig 1 Idealised DESH 3 Stage Wake

The opposed axial vorticity segments will diffusively cancel faster than this spread of azimuthal ring vorticity to infinity. So idealise the swirl to dissipate first in isolation in a new 'midwake'.

The most optimistic but plausible model would be all the expansion with the swirl undissipated for the maximum pressure regain in the near wake, followed by swirl dissipation with no further net expansion in the mid wake. No net expansion roughly requires no average guage pressure at stage 1 to match the ambient pressure at station '0'.

So the swirl (difference) is taken to decay first, giving a state '0' with just axial velocity u_0 and ambient pressure p_0. In this first dissipation the head $\frac{1}{2}\omega_1^2 r_1^2$ of the expanded swirl is lost. Then (4) gives the simple Dissipated Expanded Swirl Head DESH eqn.

$$dP/dQ = \Delta H = \rho\Omega\omega r^2 = \frac{1}{2}\rho(V^2 - u_0^2 - \omega_1^2 r_1^2) = \frac{1}{2}\rho(V^2 - u_0^2 - \omega_1 \omega r^2) \quad (7)$$

If the entire swirl behind the rotor is dissipated then this Standard Momentum (SM) has no distinct station 1 and $\omega_1 = \omega r_1 = r$ in the equations No swirl kinetic energy is regained in any expansion and all the original swirl head $\frac{1}{2}\rho\omega^2 r^2$ added at the rotor is ultimately lost. Thus the total SM head loss is Δp.

Axial Momentum Change and Generalisation

There is no net momentum change of the outside stream, so spanning where the rotortube outer pressure varies before the far wake, the net upwind force on the flow outside it produces in conjunction with the expansion of the edgestream must be balanced by the net downwind force from the ambient pressure p_0 over the end difference in area. (Thus the axially effective average of the edgestream pressure is p_0). Then in the rotortube momentum change between upstream at p_0, and downstream at p equal to p_0 at the rotortube edge, there is only an integral of the guage pressure $p-p_0$ over the downstream area. Joukowski assumed the same equation applied to each annular differential area. This implies the average wall pressure on the internal stream tubes is also p_0. Then at '0' where the pressure is constant at p_0 , the outside pressure terms vanish and

$$\rho \mathrm{d}Q\,(V-u_0) = \mathrm{d}T = \Delta p\,\mathrm{d}S \qquad (9)$$

The actuator disc Lift d$\underline{L}$ has axial component dT (9) and azimuthal component dΓr (1). Define the components of 2$\underline{\mathbf{I}}$ as the peak variations from the undisturbed wind, or axially $V-u_0$ between far upstream and downstream , but transversely as ωr the velocity jump across the rotor. Then d$\underline{L}$=2$\underline{\mathrm{I}}$ ρdQ Now dQ=udS=$\underline{\boldsymbol{\mathcal{V}}}$ •$\underline{\boldsymbol{n}}$ dS where $\underline{\boldsymbol{\mathcal{V}}}$ is the net flow u, ½ωr at the rotor and $\underline{\mathbf{n}}$ is the downwind normal of dS Now with the blades moving at speed xV on dS in the direction $\underline{\mathbf{t}}$, their apparent wind is $\underline{\boldsymbol{\mathcal{V}}}$ -$xV\underline{\mathbf{t}}$=$\underline{\mathbf{W}}$ and d$\underline{\mathbf{L}}$=2$\rho\underline{\mathbf{I}}$ $\underline{\mathbf{W}}$•$\underline{\boldsymbol{n}}$ dS (10)

Combining (9) with (7) gives $V\mathrm{d}T-\mathrm{d}P=\tfrac{1}{2}\rho\mathrm{d}Q\,((V-u_0)^2+\omega_1^2 r_1^2)$ (11)

This is the power balance in the wind frame where the gross drag power of the rotor element is the useful power removed plus the wasted flux of the kinetic energy of the axial velocity deficit [6] and the expanded swirl left behind (and ultimately dissipated) in the wake. The thrust efficiency is the ratio of the first two, and is relevant structurally and for windparks.

Anyways, substituting (3) in (9) $(\Omega+\omega/2)\omega r^2=u(V-u_0)$ (12)

or the orthogonality condition $\underline{\mathbf{I}}$•$\underline{\mathbf{W}}$=0 due to $\underline{\boldsymbol{L}}$•$\underline{\mathbf{W}}$=0 the lift $\underline{\boldsymbol{L}}$ doing no work in the viewpoint of the apparent wind $\underline{\boldsymbol{W}}$. Comparing with the head equation (7) expansion $r_t>r$ implies $\omega<\omega_1$ and so $u>\tfrac{1}{2}(T+u_0)$.

The SM head equation being $\Omega\omega r^2=\tfrac{1}{2}(V^2-u_0^2-\omega^2 r^2)$, (12) implies $u=\tfrac{1}{2}(V+u_0)$. This means that the vector induced flow at the rotor is just $\underline{\mathbf{I}}$, so the SM can be easily generalised to include blade motion at a general angle θ to the true wind. The following attempt at general justification falls a bit short, because it lacks the Hawt's $\underline{\mathbf{J}}_t$=$\underline{\mathbf{I}}_t$, due to its (unyawed) flow axisymmetry....

Since the net flow relative to the ground, $\underline{\boldsymbol{\mathcal{V}}}$ =$\underline{\mathbf{W}}$- $xV\mathbf{t}$ and $\underline{\mathbf{I}}$•$\underline{\mathbf{W}}$=0, (10) gives dP/dS =2ρ($\underline{\mathbf{W}}$•$\underline{\mathbf{n}}$)$\underline{\mathbf{I}}$• $\underline{\boldsymbol{\mathcal{V}}}$ Equate this to the loss in flow kinetic energy as it crosses the rotor segment downwind unit normal $\underline{\boldsymbol{n}}$, again ignoring any pressure deficit in the wake and assuming the peak induced flows I are entirely dissipated without regain. The change in velocity squared is $\underline{\mathbf{V}}$•$\underline{\mathbf{V}}$-($\underline{\mathbf{V}}$+2$\underline{\mathbf{I}}$)•($\underline{\mathbf{V}}$+2$\underline{\mathbf{I}}$) = -4$\underline{\mathbf{I}}$•($\underline{\mathbf{V}}$+$\underline{\mathbf{I}}$), so dP/dS =2ρ($\underline{\mathbf{W}}$•$\underline{\mathbf{n}}$)$\underline{\mathbf{I}}$•($\underline{\mathbf{V}}$+$\underline{\mathbf{I}}$) also so $\underline{\mathbf{I}}$•($\underline{\boldsymbol{\mathcal{V}}}$ -$\underline{\mathbf{V}}$-$\underline{\mathbf{I}}$) =0. Thus the component of the average induced flow $\underline{\mathbf{J}}$= $\underline{\boldsymbol{\mathcal{V}}}$ -$\underline{\mathbf{V}}$ in the direction of the (peak) velocity change 2$\underline{\mathbf{I}}$ must be $\underline{\mathbf{I}}$, as in Fig 1. So any difference $\underline{\mathbf{J}}$-$\underline{\mathbf{I}}$ in the cross-sectional plane is parallel to

W . Thus the real induced flow at the actuator $\underline{\boldsymbol{J}}=\underline{\boldsymbol{v}}-\underline{\boldsymbol{V}}$ differs from **I** only perpendicular to **I** , either insignificantly spanwise ($\underline{k}$) (implicitly in the Hawt) or in the direction of $\underline{\boldsymbol{W}}$. At large speed ratio $x=\Omega r/T$, $-\underline{\boldsymbol{W}}\to -x\underline{V}\underline{\mathbf{t}}$ and $\underline{\mathbf{J}}-\underline{\mathbf{I}}$ in this direction, will be insignificant in comparison. This generalises Glauert's kinetic energy flux argument for $\underline{\mathbf{J}}\bullet\underline{n}=\underline{\boldsymbol{I}}\bullet\underline{n}$ in his 1D Hawt limit of high x to any windmill at high x.

This general argument does not apply to the expanded swirl Hawt because the dissipated swirl component of **I** in $4\underline{\mathbf{I}}\bullet(\underline{\mathbf{V}}+\underline{\mathbf{I}})$ would be the reduced expanded one whilst for the momentum equation **I** is defined as the full swirl right behind the rotor.

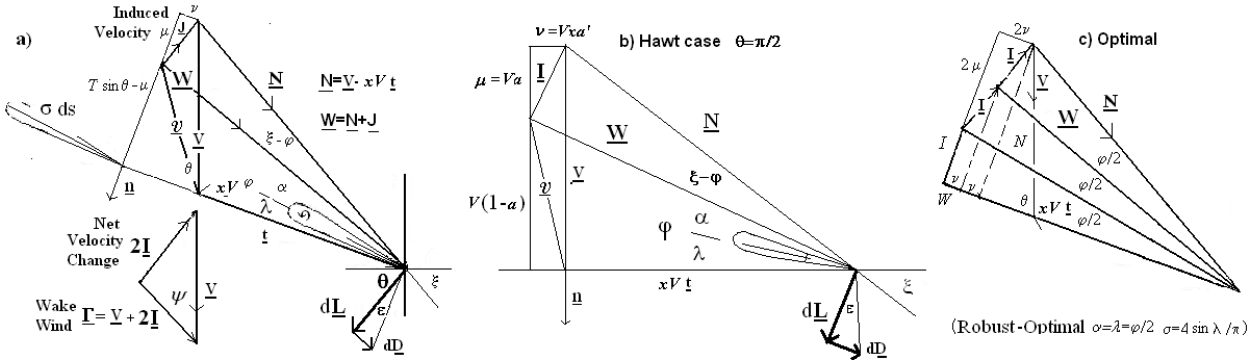

Analytic Optimum of the General Momentum Model

Add the true wind $\underline{\boldsymbol{V}}$ and the self wind $-xV\underline{\mathbf{t}}$ spanning a general angle θ, to get the undisturbed ***N***aive, ***N***ominal, or ***N***o-lift apparent wind $\underline{\boldsymbol{N}}=\underline{\boldsymbol{V}}-xV\underline{\mathbf{t}}$ at angle ξ to the path unit tangent $\underline{\boldsymbol{t}}$ in the direction of motion, unit downwind normal $\underline{\boldsymbol{n}}$. Then to form the real total blade apparent wind $\underline{\boldsymbol{W}}$ at angle φ, the induced velocity **I** perpendicular to $\underline{\boldsymbol{W}}$ from eqn (12) must be added to $\underline{\boldsymbol{N}}$, as in Fig 1. The power P is blade velocity times thrust, so from eqn (10)

$$dP/dS=2\rho xT\, v\,(\underline{\boldsymbol{W}}\bullet\underline{n}) \quad \text{with } v=\tfrac{1}{2}\omega r=I\sin\varphi, I=N\sin(\xi-\varphi),\ \underline{\boldsymbol{W}}\bullet\underline{n}=W\sin\varphi,\ W=N\cos(\xi-\varphi) \quad (13)$$

$$\therefore\ dP/dS=\rho\, xV\, N^2\sin^2\varphi\sin 2(\xi-\varphi) \quad (14)$$

Defining the Vawt normal interference $a=\boldsymbol{I}\cdot\boldsymbol{n}/\boldsymbol{V}\cdot\boldsymbol{n}=\mu/V\sin\theta\to 1-\phi/\xi$ generalizes $m=1/x\to 0$ and $\xi\to m\sin\theta$ limit of equation (14) Glauert's 1D momentum equation:

$$dP/dS\to 2\rho(\boldsymbol{V}\cdot\boldsymbol{n})^3(1-a)^2a+O(m\cos\theta, ma) \quad (15)$$

$\boldsymbol{V}\cdot\boldsymbol{n}$ generalizes $V\sin\theta$ to discard any spanwise component of $\boldsymbol{V}$ in the Darrieus 'catenary' Vawt . with the optimum limit value of $8\rho(\boldsymbol{V}\cdot\boldsymbol{n})^3/27$ at $a=1/3$

The φ derivative of dP/dS in (3) is $2\rho xVN^2\sin\varphi\sin(2\xi-3\varphi)$ vanishing at the best $\underline{\varphi=2\xi/3}$ (16)

So the optimum **angular** interference $1-\varphi/\xi$ is 1/3 at **all** x, and all θ that have $\underline{\boldsymbol{J}}=\underline{\boldsymbol{I}}$. the (peak)

At the optimum (16) $d^2(dP/dS)/d^2\varphi$ is $-6\rho xVN^2\sin\varphi$ (17), dP_O/dS is $\rho xVN^2\sin^3\varphi$. (18)

Dividing gives a peak half width squared of $\sin^2\varphi/6$ which compared with the scale φ^2 to the zeroes of dP/dS indicates a relatively sharper peak at large ξ or small x.

Reflecting $\underline{\boldsymbol{N}}$ about $\underline{\boldsymbol{W}}$ as in Fig 1c then shows optimally $I/V\sin\theta=1-2a=1/(1+2\cos\varphi)$ (19)

since $\mu=I\cos\varphi$, where $a=\mu/V\sin\theta=\cos\varphi/(1+2\cos\varphi)$. Inverting discovers $\cos\varphi=a/(1-2a)$ (20)

wake/rotor area $(1-a)/(1-2a)=1+\cos\varphi$, $W=W\cos\varphi+v$ now $xa'=v/V\sin\theta=\sin\varphi/(1+2\cos\varphi)$ (21)

For Hawt $\theta=\frac{1}{2}\pi$, W is also $xV+2v$ so $a'=(1-\cos\varphi)/(2\cos\varphi-1)=(1-3a)/(4a-1)$ (22)
So $x=\sin\varphi(2\cos\varphi-1)/(1+2\cos\varphi)(1-\cos\varphi)$ is proved an identity for $x=\cot(3\varphi/2)$ (23)
In the high x small φ limit then the circulation $x^2a'\to 2/9$. Expansion at large x gives
$c_{PO}=dP_O/dS/\frac{1}{2}\rho V^3=16(1-2/9x^2+..)/27$ Fig 5 uses (18) and (23) to graph c_{PO} vs x

GM optimum tip

Prandtl [3] considered the induced flow around the vortex sheets trailing from the B blades at relative velocity $\boldsymbol{W}$, angled at tip Φ, and spaced at $s=2\pi\sin\Phi\, r/B$. He ignored the stagger of the sheets which is a greater for a windmill blade than a propellor's for the same x. They move downstream relative to the wind $\boldsymbol{V}$ at self-induced $2\boldsymbol{J}$ perpendicular to $\boldsymbol{W}$. He found $\boldsymbol{J}=\boldsymbol{I}/F$, F a function of $(R-r)/s$ as the induced flow at the blades, and showed this reduced the effective length of the blade by $.221s$. (His implicit blade circulation $cC_L W/2=2JsF$ follows F from zero at the tip to unity inboard with J and s constant. Attempts to correct his model lose this consistency).

F is .98 by the distance $s_0=2\pi\sin\varphi\ r/B$ inboard, so from there inboard the above optimum c_{p0} can be taken to apply. Outboard the power remnant is $\int 2\pi r\ dP/dS\ dr$ from $R-s_0$ to R , or $2\pi R\,(s_0-.221s(\Phi))dP(\Phi)/dS$ (24). Since smaller Φ makes smaller $s(\Phi)$, it pays to decrease Φ below the φ which just optimises $dP/dS(\varphi)$. Setting the Φ derivative to 0,
$d(dP/dS)/d\Phi\ (s_0-.221s)=.221\ dP/dS\ ds/d\Phi$. (25) Since the tip Φ is small this gives
$\Phi(2\xi-3\Phi)(2\xi/3-.221\Phi)=.221\ \Phi^2(\xi-\Phi)$ (26)which is the quadratic $.884g^2-2.663g+4/3=0$ (27)
for $g=\Phi/\xi$ with optimum $\Phi/\xi=.634$ instead of .667. Thus the optimum Φ/ξ is lowered by about .033 on average in the tip region , maybe .05 max , to shorten it.

Drag correction of GM optimum

The net force is a rotation of $d\boldsymbol{L}$ through the drag to lift angle $\varepsilon=\tan^{-1}C_D/C_L$. This drag arises by flow retardation in the boundary layer, so it does not affect $\boldsymbol{J}$, the outer inviscid flow at the B blades induced by the lift. The net power P can be expressed in terms of the angles of Fig 1 as

$dP=xV\underline{\boldsymbol{t}}\bullet(d\underline{\boldsymbol{L}}+d\underline{\boldsymbol{D}})=2\rho\,xV\ (\boldsymbol{W}\bullet\boldsymbol{n})\ I(\sin\varphi-\cos\varphi\tan\varepsilon)\,dS$ (28)

$J=N\sin(\xi-\varphi)$, $\boldsymbol{W}\bullet\boldsymbol{n}=W\sin\varphi$, $W=N\cos(\xi-\varphi)$ $dP/dA=\rho\,xV\,N^2\sin2(\xi-\varphi)(\sin^2\varphi-\frac{1}{2}\sin2\varphi\tan\varepsilon)$ (29)
To optimise for a set, ξ again zero the φ derivative of dP/dS

$\rho\,xV\ N^2(2\sin\varphi\sin(2\xi-3\varphi)-\sin(2\xi-4\varphi)\tan\varepsilon)=0$ (30)

Expanding $2\xi-4\varphi$ as $(2\xi-3\varphi)-\varphi$ gives
$2\sin\varphi\sin(2\xi-3\varphi)\cot\varepsilon=\cos\varphi\sin(2\xi-3\varphi)-\sin\varphi\cos(2\xi-3\varphi)$ (31) so $2\cot=\cot\varphi+\cot(3\varphi-2\xi)$ (32)
$\varphi=0$ is near a minimum and $3\varphi=2\xi$ near a maximum. A second approximation to the latter is
$\varphi_o=\frac{2}{3}\xi+\varepsilon/6+O(\varepsilon^2)$ or $\xi=3\varphi_o/2-\varepsilon/4$ (33) The drag effect is very weak given that typical ε are less than a degree Then the optimum **angular** interference $1-\varphi/\theta$ at the blades virtually remains 1/3 at **all** x, and all the results of sec 3 apply. With $c_p=dP/dS/\frac{1}{2}\rho V^3$

$c_{p\,o} = 2x\,N^2 \sin(\varphi_o - \varepsilon/2)\,(\sin^2\varphi_o - \tfrac{1}{2}\varepsilon \sin 2\varphi_o)$ (34)

So to a first approx the segment power just corrects fractionally as $\varepsilon \cot \varphi_o \approx 3\varepsilon x/2$ (35)

Thus Glauert's separation of the momentum lift power optimisation from the drag loss at a given x has been justifiied

Wake Expansion from the Stability Viewpoint

Refocusing on the Hawt at zero yaw, the optimal SM solutions can be checked against its assumption of wake swirl dissipation before expansion and certainly before dissipation of the axial velocity deficit. Indeed the optimum SM axial velocity peak at the hub would tend to be decreased by the slower velocity at bigger x before both are raised by the friction with the wind outside the rotortube.

Flows with swirls theoretically develop reverse flows and multiple solutions in deceleration [5] roughly when their swirl speed exceeds their axial, the experimental criterion for a vortex to burst [6]. Equating these speeds behind the SM optimal Hawt $2xa' = 1-a$ or $\tan \tfrac{1}{2}\varphi = \tfrac{1}{2}$ at local speed ratio x=.18 and in the naive wake of induced flow 2**I**, $2xa' = 1-2a$ or $\sin \varphi = \tfrac{1}{2}$ at x=1 [2].

Very detailed calculations [7] for (non SM optimal) constant circulation windmill blades confirm the blade root vortices become unstable as they diffuse into a single continuous actuator axial vortex. But it appears possible that for x above about 1 the wake maybe stable enough to allow expansion to convert some swirl into "regained" pressure head before the residual expanded swirl is dissipated. Ironically to solve these new equations requires following the algebraic and numeric method Glauert used for the SM , missing the above simple (and general) solutions...

Solution of the DESH Optimum

With $u=V(1-A)$, $u_0=V(1-2a)>0$, $y=x^2$, & expansion $e=y/y_1$, orthogonality (9) & DESH (7) give resp.

$a(1-A) = ya'(1+a')$ (36) and $a(1-a) = ya'(1+ea')$ (21) so $(1-a)/(1-A)=(1+ea')/(1+a')$ (22)

And also $a(a-A)= v^2(1-e)$ (23) so the positive $a-A$ arises only from the expansion of the swirl velocity $v= xa'$. As $x\to\infty$ x^2a' must remain finite so the right hands of (20) and (21) become identical regardless of e so $a=A$ and then optimising $c_p=4ya'(1-A)$ gives $1-3a=0$ $a=A=\tfrac{1}{3}$ and $ya' =2/9$. This outer limit of diminishing swirl takes DESH into SM and will dominate mass conservation to give $e=\tfrac{1}{2}$

To solve generally, optimise [$c_p=4ya'(1-A)$ starting with $(1-A)\mathrm{d}a'/\mathrm{d}A=a'$ (24).

Equations (20) and (21) can be differentiated to give two more relating $\mathrm{d}a'/\mathrm{d}A$ and $\mathrm{d}a/\mathrm{d}A$ at a local optimum with y and e fixed, so that elimination yields a relation between the optimal A, a,

and xa' which then can be solved simultaneously with (20) and (21). In detail,

$(1-A)\mathrm{d}a'/\mathrm{d}A=a'$ (24) $(1-A)\mathrm{d}a/\mathrm{d}A-a = y(1+2a')\mathrm{d}a'/\mathrm{d}A$ (25) $(1-2a)\mathrm{d}a/\mathrm{d}A=\mathrm{y}(1+2ea')\mathrm{d}a'/\mathrm{d}A$ (26)

Subtracting $(1-2a)$x(25) from $(1-A)$x(26) eliminates $\mathrm{d}a/\mathrm{d}A$,

$a(1-2a)=\{2a'(2a-eA)+(2a-A)+2a'(e-1)\}\ y\mathrm{d}a'/\mathrm{d}A$ (27)

Multiplying (24) by (27) by $ya'(1+a') =a(1-A)$ (29) allows cancellation of $ya(1-A)a'\mathrm{d}a'/\mathrm{d}A$ so

$(1-2a)(1+a')=\{\ \}$ (29) so solving $a'(6a+2e(1-A)-3) =(1-4a+A)$ (30)

which reduces to the standard $a'=(1-3a)/(4a-1)$ for the SM $A=a$ and $e=1$.

Solving for a' in (22) $a-A=a'(1-e(1-A)-a)$ (31) so multiplying (30) by (31) eliminates a' to give

a quadratic in a and A. $(a-A)(6a+2e(1-A)-3) =(1-4a+A)(1-e(1-A)-a)$ (32)

$2a^2+ a(2-2e(1-A)-5A) +e(1-A)^2+2A-1 =0$ (33) If $g=1-A$ $eg^2+g(a(5-2e)-2)+(1-a)(1-2a)=0$ (34)

The equations suggest a Glauert-type 'back substitution' solution such as supposing an a and e, solving for g ie A(- root), then a', and finally for x. Equations (30) and (31) are both needed for a', because (31) is indeterminate (0/0) in the $e=1$ $A=a$ SM limit, whereas at $e=¾$ equation (34) exactly solves as $a=(1+A)/4$ which makes (30) indeterminate.

The determination of e involves more complication than just awkward coupling integration out from $x=0$, because e is the local expansion ratio to station '1' not '0'. Even though there is no rotortube expansion between these two of the same average pressure, there is local variation in the expansion because the centreline fluid decelerates from suction at 1 to ambient pressure at 0, whilst the outer half of the fluid has balancing positive pressure at 0 and so accelerates.

The strategy adopted here is to try a variation of e with a (to ultimately $e=½$ at $a=A=⅓$) from one of these starting values and then integrate for the actual expansion ε from the solution, and try to adjust the e's to match ε. To specify the equations used to calculate ε, at the end of the expansion, $v_1/V=2xa'\sqrt{e}$ $dp/dx_1=\rho v_1^2/x_1$ so integrating by parts for no net pressure gives for $\mathrm{p}_1=(p_1-p_0)/\frac{1}{2}\rho V^2$, $y_1=y/e$

$P_1\ Y_1 =\int(v_1/V)^2\, dy_1$ and then $\mathrm{p}_1=P_1-\int(v_1/V)^2\, dy_1/y_1$ $u_1/V=\sqrt{(1-2a)^2}-\mathrm{p}_1$ $y_1/\varepsilon=\int(1-A)V/u_1\, dy$ (36)

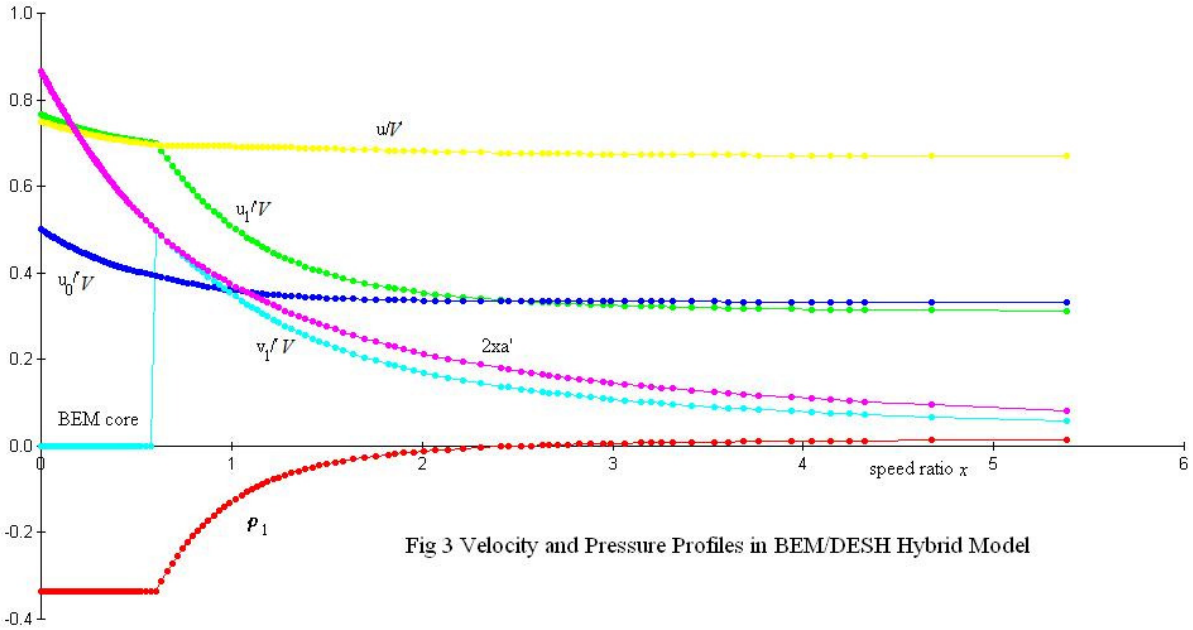

Fig 3 Velocity and Pressure Profiles in BEM/DESH Hybrid Model

where P_1 and Y_1 are the tip values. The slight net recontraction from 0 to 1 could be iterated out by dropping P_1 slightly closer towards p_0 .

Generally the difference between e and ε can be eliminated except in a region of small x<1 where ε invariably exceeds 1 due to the strong u_1 at small x_1 due to the (singular) suction there.

Hybrid Optimal SM-DESH

This suggests a hybrid model (Figure 1) which ignores the swirl and radial pressure gradient at '1' in a core zone on the conjecture that the clearly unstable swirl near the rotor axis is already dissipated or exported by vortex bursting. This very much limits the small x rise of u_1 and ε (into contraction) so that e and ε are essentially matched at 1 in this SM core zone of dissipation before expansion. The transition to non-zero v_1 and DESH then can be made at x=.57. The expansion of the core region is then delayed to between stages 1 and 0, when the interface suction can decline with the dissipation of the outer swirl. This agrees with CFD calculations showing about a rotor diameter long zone downwind of a streamlined nacelle before the central wind diminishes[12]. The higher 'turbulence' intensity level in the CFD wake suggests an instability such as vortex bursting.

The small angular momentum of the core must transfer outwards in the burst, but its small addition to the DESH zone swirl will be ignored, just as has any radial transfer of axial momentum always been. It should be emphasised that the features of interest develop as e drops significantly into expansion typically at x>1. Figure 3 shows the velocities at all three stations as well as p_1, the non-dimensional pressure at station 1. Note how slight the p_1 is on the tip streamline, about the reverse of the x=2 value. Here u_1 exceeds v_1 everywhere by a minimum of 40% stability margin downwind of the rotor. This happens to coincide with the .6 upper limit

of tangential to axial velocity observed by Masouh[8]. Medici [10] measured a broad midblade peak of swirl velocity at 1 m/s with axial velocity 4m/s under-reduced from the true wind 8m/s at the same 1 diameter downstream with only weak rotation near the axis.

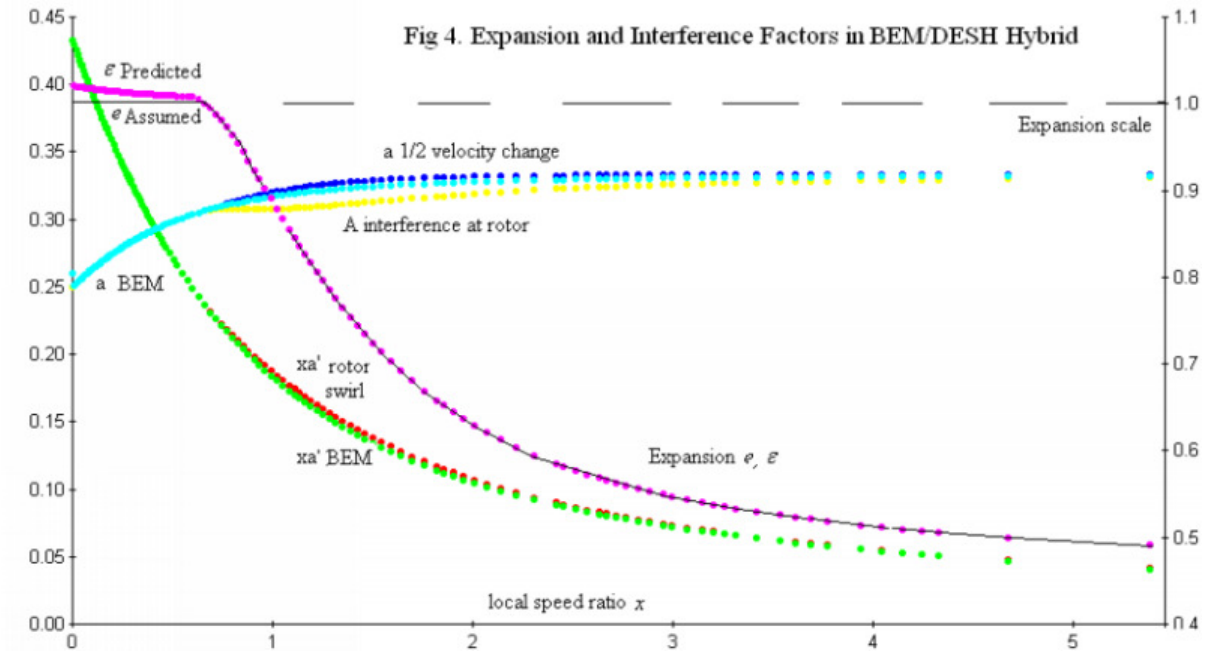

Fig 4 shows the main differences in the rotor flow vs the all-SM optimal are the increase in xa' by about 3% due to the lower swirl penalty and lowering of the interference A at the rotor by about .013 peak whereas a, half the wake net velocity change only rises slightly. So the expansion from far upwind to stage 0 is virtually unchanged , but slightly more of this occurs downstream. The difference a-A is about .02 reducing to zero at the tip consistently with thevortex picture, and close to CFD[13] and ring vortex [4] calculations for constant A=⅓. The changes raise the thrust coefficient $c_T=4a(1-A)$ over the SM by a peak of 3.2% at about x=1.35, to an absolute peak of 905 at x=1.6 vs the SM asymptote of .89. The increase in 1-A dominates the increase in $1+a'$ so tan $\varphi = (1-A)/x(1+a')$ is increased by peak 1%.

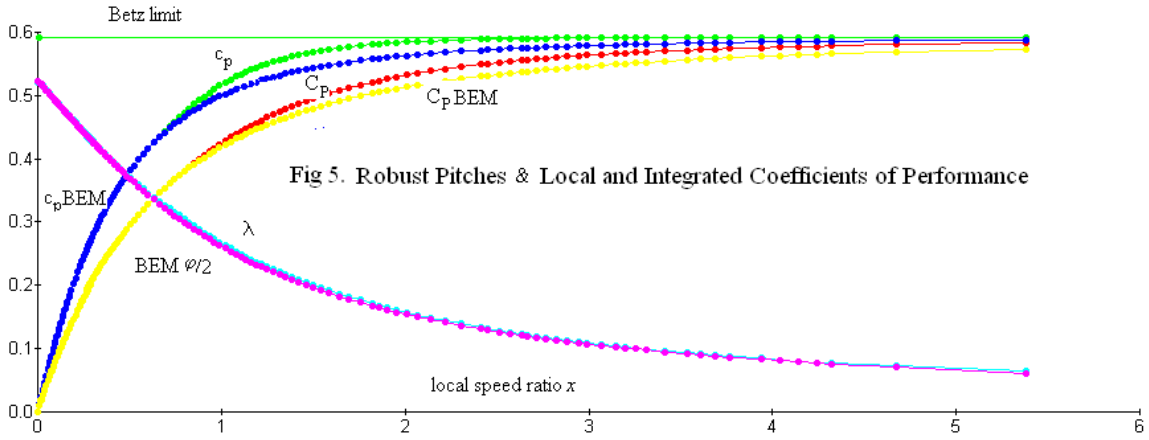

Figure 5 shows the difference in local c_p from the Betz limit is more than halved from x=1.5 on

and the greatest absolute difference of c_p is about .025 at x=1.5. Of this 4.6% increase, 3% comes from the swirl increase directly and 1.6% from the increase in $(1-A)$, the flux at the rotor. The net improvement in local thrust efficiency is about 1.5% peak. The local power virtually obtains the Betz limit by x=2. These results are for X=5.5, but values at a given x are only weakly affected by X, e.g. $c_p(1.5)$ is increased by only .3% for X=3.5. So it is a good approximation to just integrate the $c_p(x)$ at middle X=5.4 to get $Cp(X)$. An increase peaking at about .019 or 3.5% is seen to broadly span X=1.5 to 3.

Chapter Conclusion

Glauert's original momentum optimisation has been solved in general as angular interfence of 1/3 and the tip and drag corrections have been shown to be small. Even perfect flow expansion has a fairly small net effect on the lift, limited by the lack of swirl to partially regain at the tip and its instability near the root.

Chapter 2 Optimal Blade Elements

It is a separate dependent problem to the above momentum optima what the blade chord and pitch should be versus x. The lift on the B blades each of chord c for solidity $\sigma=Bc/2\pi r$ must match the momentum lift (10). If $\underline{r}$ is the unit radius, $\underline{\boldsymbol{W}}$ is the apparent wind, magnitude W, angle φ to tangential the blade element (momentum) equation is

$$\tfrac{1}{2}\rho W C_L \underline{r} \times \underline{\boldsymbol{W}}\, \sigma dS = -d\underline{\boldsymbol{L}} = 2\rho \underline{\mathbf{I}}\ (\underline{\boldsymbol{W}} \bullet \underline{\boldsymbol{n}})\, ds \qquad (1) \qquad \tfrac{1}{4}\sigma C_L = I\sin\varphi / W = v/W \qquad (2)$$

With $v/W = 1-\cos\varphi = \sin\varphi \tan\tfrac{1}{2}\varphi$ for optimal GM; so with $k=\Omega c/T$, then $BkC_L/2\pi = 4xv/W$ (3)

So at $\theta=\pi/2$ for optimal GM $BkC_L/2\pi = 4(1-\cos\varphi)\cot 3\varphi/2 = 4(2\cos\varphi - 1)\sin\varphi/(2\cos\varphi + 1)$ (4)

which peaks at $\varphi=35.5^{o}$ or $x\approx\tfrac{3}{4}$ as revealed in Fig 6.

The DESH increase in swirl increases v/W so in Figure 6 the optimum $BkC_L = 8\pi xv/W$ is increased by about 2.5% with the peak difference at x=1.5, where subscript s denotes stall value.

Not this only specifies the product of blade chord and lift coefficient. Glauert selected the lift coefficient of smallest ε to minimise the drag correction at optimum. So then the chord followed the above shape. But this does not account for the great variability of the wind, and the annual power is better optimised by making the windmill maintain optimum for at least small variations of the wind...

Robustly Optimal Blade Elements

Prior to stall $C_L=2\pi sin\ \alpha$ where α is the ¾ chord angle of attack or φ.-λ, the blade pitch angle. So with $\varpi=\pi\sigma/2=Bc/4r$, (2) is $\varpi\sin\alpha = v/W$ or GM $\varpi\sin\alpha = sin\varphi\ tan(\xi-\varphi)$ (5) or for the GM optimum. $\varpi\sin\alpha=(1-\cos\varphi)$ (6)

Then, for a blade element to robustly remain optimal at its fixed $\Omega,c,r,\varpi,\lambda$ as the windspeed varies the angle ξ and so φ in proportion, requires $\varpi\cos(\varphi-\lambda)=d(v/W)/d\varphi$. (7) or $\sin\varphi$ for the GM. Then dividing into (6) gives GM $\tan(\varphi-\lambda)=\tan½\varphi$ so $\alpha=½\varphi=\lambda_r$ (8) completing the exact optimal GM trisection of ξ_d into $\lambda, \alpha_d, ½\varphi_d$ with $\varpi=2\sin\alpha_d \uparrow \varphi_d$ (9) or $Bk\rightarrow 8/3$. To avoid the C_D of leading edge separation of small sheet metal blades, such thin circular arcs should be set like jibs to have no chordal angle of attack at φ_d. To make this optimum robust, their trailing edges at twice the ¾ chord α_d should be at φ_d from ***W*** or just parallel to the motion.

In general $\tan(\varphi-\lambda)=v/W\ d\varphi/d(v/W)$, differentiated numerically for the DESH optimal v/W and φ vs x to find the robust λ. Then (5) can be solved for Bk as graphed versus the simple GM robust $\lambda=½\varphi$, $\varpi=2\sin\lambda$ [2]. Figure's 5 and 6 show that relative to BEM, the DESH increase in BkC_L/C_{LS} would be met by a proportionate rise in chord Bk because the angle of attack $\alpha=\varphi-\lambda$ is little changed as the slight growth in φ is matched by the change in robust pitch λ. So the design robust chord and pitch are bigger. With the $\alpha_S=20^o=.35$ (enhanced over static by the centrifuging in the boundary layer) of Figure 6, the plots of the robust Bk falls slightly below the plots of BkC_L/C_{LS} implying slight jogs in the best blade profiles on account of stall. (A super-enhanced stall of 26^o would make the robust rule for all x). In reality bending strength will require bigger hub thickness and so chord for cantilever blades, as well as curtail the outer chord and pitch to limit the absolute torque at high T and low X.

Drag, lift slope and tip corrections

With the Prandtl tip factor F, the BGM equation becomes $\sigma C_L=4F\sin\varphi\tan(\xi-\varphi)$ (10)

At modest ¾ chord angle of attack α, $C_L/2\pi=e\sin\alpha$, where e is a thickness factor slightly decreasing the theoretical lift slope. Since (1.) gives optimally $\xi-\varphi_o=½\varphi_o-¼\varepsilon$, then

$\varpi\sin\alpha=F\sin\varphi\tan(½\varphi_o-¼\varepsilon)$ (12) if $\varpi=½e\pi\sigma=eBc/4r$ for B blades each of chord c.

For this to robustly hold the optimum despite φ_o varying with θ about φ_d at set ϖ and λ requires

$\varpi\cos(\varphi_o-\lambda_r)=F\cos\varphi_o\tan(\xi-\varphi_o)+(\tfrac{1}{2}-\tfrac{1}{4}d\varepsilon/d\alpha)\,F\sin\varphi_o\sec^2(\xi-\varphi_o)+\sin\varphi_o\tan(\xi-\varphi_o)dF/d\varphi_o$ (13)

since the rotor tip φ, Φ will change too. Dividing equations (13) by (12) at φ_o gives

$\cot\alpha_r=\cot\varphi_o+(1-\tfrac{1}{2}d\varepsilon/d\alpha)\csc(\tfrac{1}{2}\varphi_o-\tfrac{1}{4}\varepsilon)+dF/Fd\varphi_o$ (14)

Taylor expanding the second term gives

$\cot\alpha_r\approx\cot\tfrac{1}{2}\varphi_o+\tfrac{1}{2}\varepsilon\csc\varphi_d\cot\varphi_o-\tfrac{1}{2}d\varepsilon/d\alpha\csc(\varphi_o)+dF/Fd\varphi_o$ (15)

Well inside of the tip $dF/d\varphi_o=0$ and then Taylor expanding $\cot^{-1}$ of the right side gives

$\alpha_r\approx\tfrac{1}{2}\varphi_o-\varepsilon(1-\tan^2\tfrac{1}{2}\varphi_o)/8+\tfrac{1}{4}d\varepsilon/d\alpha\tan(\tfrac{1}{2}\varphi_o)+O(\varepsilon^2)$ (16)

So $\alpha_r\approx\tfrac{1}{3}\xi-\varepsilon/24$, showing drag to little perturb the trisection. The $dF/Fd\varphi_o$ term is simplest to evaluate by taking $s=2\pi\sin\varphi_o\,r/B$ as commonly used.

Now $\cos(\pi F/2)=e^{-f}$, so $\pi\,dF=2\cot(\tfrac{1}{2}\pi F)df$ $f=\pi(R-r)/s=B(R-r)/2r\sin\varphi_o$ so $df=-f\cot\varphi_d\,d\varphi_o$

$\cot\alpha_r=\cot\varphi_o+(1-\tfrac{1}{2}d\varepsilon/d\alpha)\csc(\varphi_o-\tfrac{1}{2}\varepsilon)-2f\cot(\tfrac{1}{2}\pi F)\cot\varphi_o/\pi F$ (17)

Using small angle approximations for α_r and φ_d appropriate at the tip's large X

$\alpha_r\approx\tfrac{1}{2}\varphi_o/h,\ h=1+\tfrac{1}{4}\varepsilon/\varphi_o-\tfrac{1}{4}d\varepsilon/d\alpha-f\cot(\tfrac{1}{2}\pi F)/\pi F$ (18)

At the very tip in the limit of small f, $2f=(\tfrac{1}{2}\pi F)^2$ so the last term in (18) tends to $-\tfrac{1}{4}$, reflecting the ½ exponent of potential flow around an edge [5]. Then $h\approx 3/4+\tfrac{1}{4}\varepsilon/\varphi_o+O(\varepsilon^2)$

Throughout, the robust ϖ_r is given by $F\sin\varphi_d\tan(\tfrac{1}{2}\varphi_o-\tfrac{1}{4}\varepsilon)/\sin\alpha_r$ (19)

So the robust blade reduces its chord by ¾ F very near the tip from the constant chord beyond the tip region (when the drag correction is ignored.)

(SM) robust attributes

Robustness allows the Hawt to remain optimal with small spatial variations in ξ over the blade path due to vertical gradients in wind speed, most significant for large wind turbines on relatively short towers. If gusts vary slowly in r/T, the time scale for passage through the rotor, the c_P stay optimum with time, so especially for small windmills.

The robust c_P has a very broad optimum. Its $\varphi-\varphi_o$ is zero and stationary in ξ at the design ξ_d with a Taylor series beginning with the square of variations $\delta\xi$, negatively as seen from the

feathering limit $\xi=\varphi=\lambda$. Since the expansion of c_P about its optimum for any ξ likewise begins with the square of $\varphi-\varphi_o$, the combined expansion is a weak quartic $O(\delta\xi)^4$ whereas for non-robust blade angles and solidities it is a stronger quadratic decrease $O(\delta\xi)^2$ ....

The robust off-peak $\varphi>\varphi_o$ $a<1/3$ benignly helps avoid high downwind induced drag $dE=2\rho\{\mu(V\sin\theta-\mu)\}\,ds \rightarrow 2\rho(1-a)a(V\sin\theta)^2 ds$ and structural loads away from the main power design point. The thrust efficiency $\eta=dP/V\,dE$ or $\tan\varphi/\tan\xi$ for a Hawt, is the ratio of useful to total power removed from the wind and so an upper limit on wind farm capture.

For $\theta=\frac{1}{2}\pi$ and small m compare GM tangent $\lambda=0$ $\varpi=\kappa=\xi_d/3$ $\alpha=\varphi=2\kappa$ and robust optimal $\varpi=2\kappa$ $\alpha=\lambda=\kappa$ element designs... For the tangent $\alpha=\varphi$ cancels in eqn (16), reducing it to $\xi-\varphi=\varpi=\kappa$. So if ξ is doubled to 6κ, say by halving x, the tangent gets $\alpha=\varphi=5\kappa$. But for the robust the quadratic (16) must be solved yielding $\xi-\varphi=1.55\kappa$, which "under-induces" less versus the ideal $\varphi=2\xi/3$. The c_P as $(1-\varphi/\xi)(\varphi/\xi)^2$ eqn (11) are reduced by .78 and .96 respectively, the loss ratio slightly exceeding the ratio of the above $(\varphi-2\xi/3)^2$. Yet the difference in stall margin in favour of the robust $\varphi=4.45\kappa$ has increased to $5\kappa-3.45\kappa=1.55\kappa$ from κ So the tangent under-induces to exacerbate its higher design angle of attack for a much earlier stall. And if ξ is

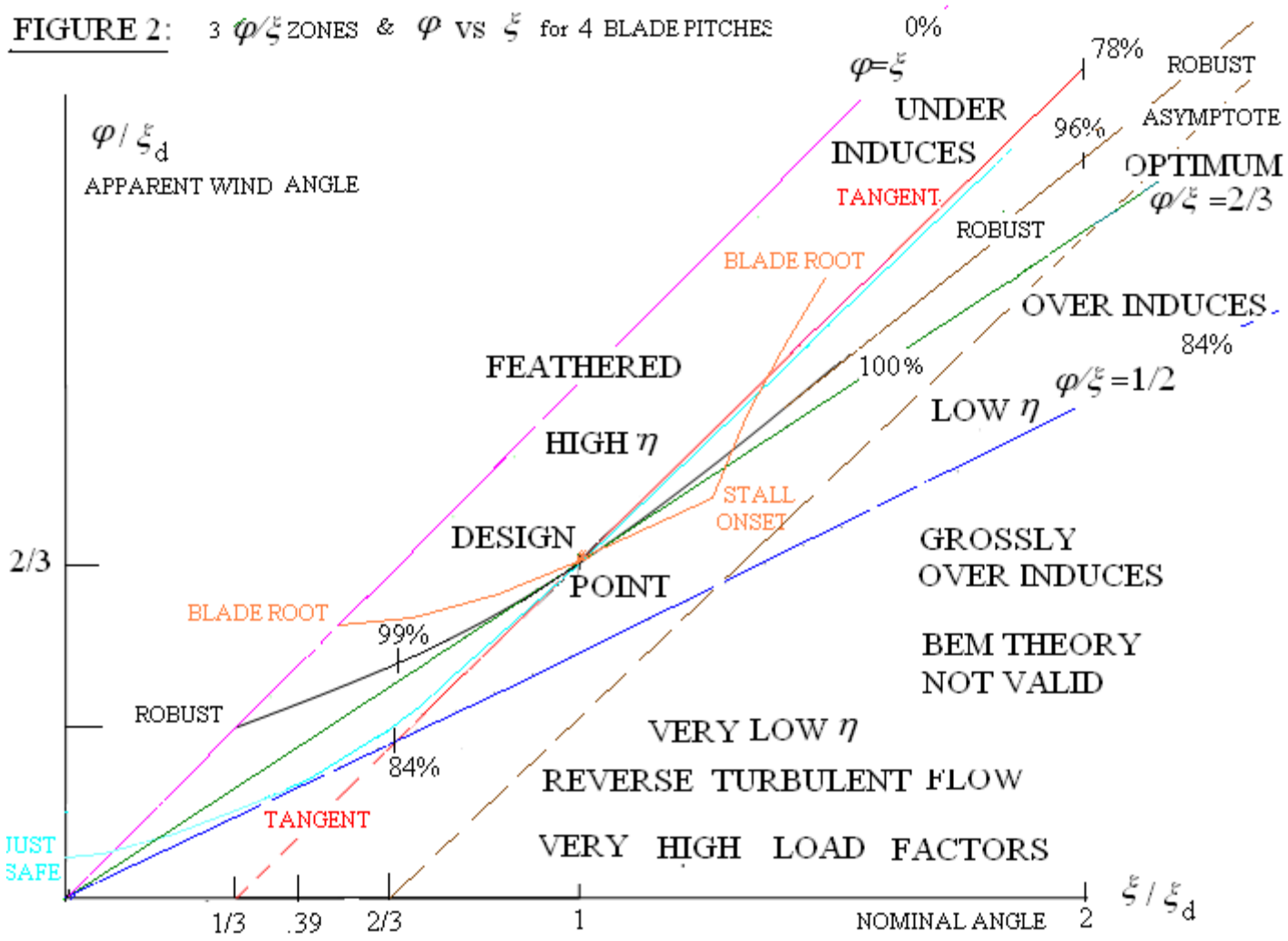

reduced to 2κ; robustly $a=1-\sqrt{½}=.29$ safely and slightly lower than optimal ⅓ with c_P ratio .99, but for the tangent c_P ratio .84 at $a=½$. This is the threshold of 'turbulent' [1] 'over-induced' reverse flow in the wake with heavy E at low c_P and so very low η. Fig 2 combines these results, showing how the robust operating curve kisses the high η side of the optimum $\varphi=2\xi/3$ line at the design point. The only price of the robust design is the higher profile drag penalty from the higher chord, which the next section will show is minor. Moving inwards on the Hawt blade $\alpha=\xi_d/3$ will stall at α_s, at about x=1. If the blade were designed just at this stall C_L peak, then eqn (12) gives $d\varphi/d\xi=2/(2-\cos\varphi)$ just above so that its operating curve would rapidly rise away from optimum. Since inner blade benign η is not of any structural significance, the ideal α_d is less than stall to get the operating line closer on average to optimum with the tradeoff of feathering at a higher low ξ, as sketched in Fig 2

5 APPLICATION TO FIXED PITCH HAWTS

Small blades are very strong for their weight and can furl to regulate or simply withstand the steady and productive loading of a near robust broad C_P peak, and they benefit most from its indifference to wind fluctuations of longer time scale than their small r/T. Raising the outer chord above the robust chord increases the zero rpm stalled blade torque for self starting. Whereas lower drag and chord blades more tangent than the robust may fatigue with the high rpm in unproductive turbulent over-inducing in high winds, as most off-grid loads are too weakly varying with Ω to prevent ξ decreasing with windspeed. At most their interference should kiss ½, the threshold of reversed wake flow, at some $\xi_{1/2}$ below the design. The small angle GM equation (5) $\varpi(\varphi-\lambda)=(\xi-\varphi)\varphi$ gives this minimum 'just safe' $\varpi = \xi_{1/2} = 0.39\ \xi_d$ versus robust $\varpi = 2\xi_d/3$. Such hyperbolae in Fig. 2 are asymptotic to the negative ξ axis.

Whereas grid-connected large Hawts can use synchronous generators to start and to yaw and to hold their rpm very constant. Because of the power penalty and need to restrict loadings, these Hawts run with high yaw variances, but it will turn out that tangent blades should be on the tangent side of robust to lose the least power in yaw. A near robust (tip) solidity produces too much absolute bending moment above the design wind, so the outer chord c, pitch λ, and section stall(3/4 chord) angle of attack α_s is reduced not only to lower the profile drag but more to deliberately prompt stall at high V and constant _ near the tip [**7**]. The constant rpm means such more tangent tips are safe in overinducing in lighter, much less powerful winds below design.

Robust SM with drag and tip correction for small wind turbines AIAA paper with alot of notation changes

The drag correction to the BEM [14] does reduce the robust chord Bk slightly with large x, before the Prandtl correction[1] tapers down the mean interference for a more gradual transition to the outer flow, rounds off the tip , and lowers the tip robust pitch λ [14].

Vortex element Hawt yaw corrections in the high speed ratio limit

To minimise dynamic loadings to compensate for the gravity loads that grow disportionately with their size (and to avoid slip rings) large Hawts sparingly use grid power to yaw slowly in response to long term persistent windshifts. Consequently they are typically operating at sizeable yaw angles, so this condition needs further analysis. Call the yaw angle γ of the rotor upwind axis γ. A first expected limit is that whatever the actuator inside the disc the yawed power must decrease at least as fast as $\cos\gamma$ the projected swept area. The component of the wind not normal to a rotor is a combination of inconsequential radial along the span of the blades or oscillatory azimuthal insignificant vs xV for large speed ratios . So the normal component alone matters with tan ξ=cosγ/x and the GM gives the power as the $\cos^3\gamma$ φ, $\underline{\mathbf{J}}$=$\underline{\mathbf{I}}$=⅓$V\cos\gamma$ normal and uniform around the azimuth. Consider the wake implications. ...

The wake velocities then angle **progressively** away from the wind in the opposite direction to the yaw. This angling should reduce the induction at the rotor and deviate it towards the wake flow axis. The vortex rings shed from the edge of the actuator disc will be further counterotated as the wake curves, further reducing their induction. The curvature also implies a crosswind pressure gradient to bend the wake which provides a net force in the momentum balance of the flow tube between upwind and downwind. Also to the extent there is residual core swirl vorticity in the deflected wake, its induction will introduce a variation of $\underline{\mathbf{J}}$ at the rotor according to the direction of rotation.

The wind that has not gone through the rotor must potential flow over the skewed wake vortex tube. Likewise downstream Batchelor [11] gives the **net rotor** lift perpendicular to $\underline{\mathbf{V}}$ as perturbing the potential stream flow outside the (diffusive) wake zone to the order of the inverse of lateral distance squared.

One common if drastic approach is to consider the rings in the far wake to be so rotated at typical γthat the induced flow comes entirely from the near wake at the initial skew angle χ it emerges from the rotor. Then the near wake can be analysed with the rings still parallel to the rotor plane They induce flow halfway between the rotor axis and the wind direction , bisecting the skew angle[ ] (So the induced flow is no longer GM, parallel to the rotor force which is

normal to the rotor.) Taking the rotor axis component of induced flow to be $AV\cos\gamma$, then the net rotor flow $\underline{\mathcal{V}}$ components relative to this axis define the skew angle :

Tan $\chi = V(\sin\gamma - A\cos\gamma\tan\chi/2)/\ V\cos\gamma(1-A) = (\tan\gamma - A\tan\chi/2)\ /(1-A)$ with the approximate small angle solution $\chi = \gamma/(1-A/2)$. Alternatively this matches the potential flow slip over the top of the wake cylinder $2V(\chi - \gamma)$ to the resolved axial velocity jump into the wake $AV\chi$ right behind the rotor.

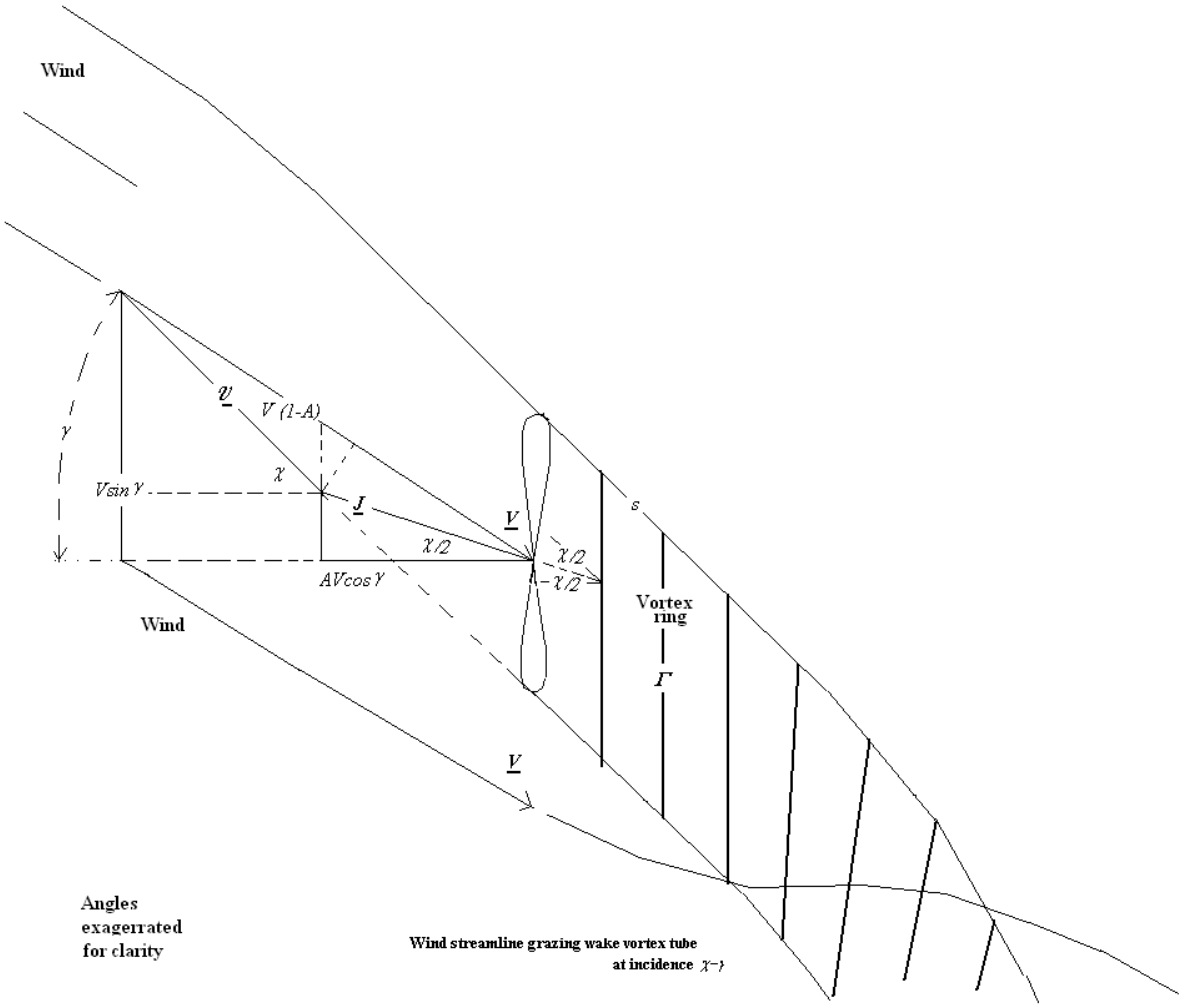

The ring spacing along the vortex tube is $s = \mathcal{V}2\pi/B\Omega$. Then if the blade circulation and so ring strength is Γ, then Coleman gave the average wake axial and so twice the rotor normal components of induced flow as Γ/s. i.e. $\Gamma = 2A\cos\gamma\ V\ \mathcal{V}2\pi/B\Omega$. Now with the high speed ratio x the blade lift per unit span is $\rho xV\Gamma$ at thrust angle $(1-A)\cos\gamma/x$ working at speed xV for a power per unit span of $\rho xV^2\ \Gamma\ (1-A)\cos\gamma$ or $2\rho V^3\ (1-A)\cos^2\gamma\ A\ \mathcal{V}2\pi x/B\Omega$. Because $x = \Omega r/V$,

then the power per unit swept area from all the B blades is $2\rho V^2 A\ (1-A)\cos^2\gamma\ \mathcal{V}$ like the BEM except $\mathcal{V}$ appears instead of a $V(1-A)\cos\gamma$. The latter is an underestimate in neglecting the benefit of the off-normal components of the wind in stretching out the wake and weakening its induction. $V(1-A)$ is closer and gives the measured $\cos^2\gamma$ power [Medici 4.13] An even closer underestimate is $V(1-A\cos\gamma\cos(\chi/2-\gamma)/\cos(\chi/2)) = (1-A)V(1+\gamma^2/5)$ approximating the optimum A as still 1/3. This gives the power to vary slightly less as $1-4\gamma^2/5$. Coleman found A to oscillate fractionally as tan $(\chi/2)$ with azimuth there is strictly a further mean square correction $\gamma^2/50$. (More importantly this indicates a slight yaw reducing moment.)

For each blade, $\Gamma=\pi x V c\ (2\cos\gamma/3x-\lambda)$ a perfect match for $\mathcal{V}=2V/3$ for tangent blades $\lambda=0$ and $Bk=4/3$. With the perhaps more accurate wake $\mathcal{V}$ the match would require $Bk=4/5$ and $\lambda=-4/9x$ (vs $\varphi=2/3x$). To the extent that the match can't be sustained, the performance would drift below optimum $1-.78\gamma^2$ towards the measured $\cos^2\gamma$ as the yaw is changed from the design and explaining the variability with rotor type Medici observed. Whereas to keep optimal as wind speed changes need substantial (robust) positive pitch. So there must be a tradeoff for best pitch according to the statistics of wind speed and direction and yaw response.

<u>Nomenclature</u>:

a' the azimuthal interference factor
a half the net axial velocity change
A the axial interference at the rotor
B the number of blades
c the local blade chord
c_P local elemental power coefficient per strip of swept area
c_T local elemental thrust coefficient = Thrust/ $1/2\rho V^2$/ unit swept area
C_L lift coefficient $L/2\rho V^2$/ unit blade area
C_P rotor coefficient of power / undisturbed kinetic energy flux through the swept area
T- the rotor downwind thrust
e the streamtube area at the rotor vs its area at station 1
f the ratio of azimuthal induced flow to apparent wind at the rotor v/W
k reduced frequency $\Omega c/V$
P the dimensional power per unit length of span
p the absolute pressure
p_1 non-dimensional gauge pressure at station 1 $(p_1-p_0)/\frac{1}{2}\rho V^2$
P_1 tip value of "
Q streamtube volume flux

Vwindspeed
$t = 1-A$ non dimensional axial velocity at rotor
W speed or magnitude of the apparent wind
u axial velocity at the rotor, behind with subscript
v azimuthal velocity behind the rotor
x local speed ratio $\Omega r/V$
X the tip speed ratio
y square of x
r unit radial vector
I the induction, half the velocity change the blades produce downstream in their wake
L airfoil lift vector
V True undisturbed wind vector
W The net apparent wind
α - ¾ chord angle of attack to **W**
α_{stall} the (dynamic) stall onset value of α
η - Glauert thrust efficiency c_T/c_P
φ - The true or complete apparent wind **W** angle to the blade path
λ - the blade pitch or angle of the 3/4 blade chord to the blade path
κ - $a'x^2$ circulation normalized by $2\pi T^2/\Omega$.
ρ fluid density
σ - true local solidity = blade chords/circumference of blade travel $Bc/2\pi r$
$\varpi = \pi\sigma/2 = Bc/4r$ half the net blade chord divided by the diameter
Ω- angular velocity of rotation in radians per unit time
subscript 0 denotes value in wake after swirl has dissipated station '0'
1 denotes value in wake at end of rotortube expansion station '1'
References

1. Glauert, H., 1935 Airplane Propellors *Aerodynamic Theory* **3** Division L (ed.W.F. Durand), J. Springer, Berlin, reprinted by Dover Publications New York 1963 TL 570 D865 (1935)

2.Farthing, S. P., "Optimal Robust and Benign Horizontal and Vertical Axis Wind Turbines" Journal of Power and Energy Vol 221 No. 7 2007 p971-979

3. Sharpe, D.J. "A General Momentum Theory applied to an Energy-Extracting Actuator Disc" *Wind Energy* **7**, 2004 pp 177-188

4. Crawford, C. "Re-examining the Precepts of the BEM Theory for Coning Rotors", *Wind Energy* **9,** 2006 pp 457-478

5. Batchelor, G.K. "Steady Axisymmetric Flow with Swirl" p543-555 in his

An Introduction to Fluid Mechanics Cambridge University Press 1967

6. Harvey, J.K. "Some Observations of the Vortex Breakdown Phenomenon" *Journal of Fluid Mechanics* **14** 4 1962 p585-593

7. J H Walther et al "A numerical study of the stability of helical vortices using vortex methods" *J. Phys.: Conf. Ser.* **75** 2007 (16pp) http://www.iop.org/EJ/abstract/1742-6596/75/1/012034

8.F Massouh *et al* "Exploration of the vortex wake behind of wind turbine rotor" *J. Phys.: Conf. Ser.* **75** 2007 (9pp) http://www.iop.org/EJ/abstract/1742-6596/75/1/012036

9.Corten, G.P. "Heat Generation by Wind Turbine" *14th IEA Symposium on Wind Turbine Aerodynamics* NREL, Colorado 2000 www.ecn.nl/rx01001.pdf

10 . Medici,D. "Wind Turbine Wakes - Control and VortexShedding". *Lic thesis* KTH. 2004www.vindenergi.org/Vindforskrapporter/Medici_2004_Wakes.pdf

11. McCutchen C.W. "A Theorem on Swirl Loss in Propeller Wakes" *Journal of Aircraft* (AIAA) 1985 22 #4 p344-346

Let $\Delta\lambda=\lambda-\lambda_{r=}\alpha_r-\alpha_d$ and $\Delta\varpi$ be small deviations from robust values. Then for the same $\varpi\sin(\varphi-\lambda)$ at $\varphi=\varphi_o$ one must have $\Delta\varpi=\Delta\lambda\varpi_r\cot\alpha_r$. Differentiating the non-optimal linear lift BEM $\varpi\sin(\varphi-\lambda)=F\sin\varphi\tan(\xi-\varphi)$ (20)

$$d\varphi/d\theta=F\sin\varphi\sec^2(\theta-\varphi)/\{F\sin\varphi\sec^2(\theta-\varphi)-F\cos\varphi\tan(\xi-\varphi)+dF/d\varphi\sin\varphi\tan(\theta-\varphi)+\varpi\cos\alpha\} \quad (21)$$

Call this u/v to be evaluated at the central design point $\varphi=\varphi_o$. Now if ϖ and λ are robust then it must be $d\varphi_o(\theta)/d\theta$, so any variation must be due to non-robust $\varpi\cos\alpha$ in the denominator. The robust denominator v in (22) must and does simplify eventually but the exercise can be avoided using the known robust values of u/v and u

$$d(\varphi-\varphi_o)/d\theta\approx-(d\varphi_o/d\theta)^2\Delta(\varpi\cos\alpha)/u \quad \text{now } d\varphi_o/d\theta=2/3,\ \Delta(\varpi\cos\alpha)=\varpi\Delta\lambda/\sin\alpha \ \&\ u=F\sin\varphi\sec^2(\theta-\varphi) \quad (22)$$

$$d(\varphi-\varphi_o)/d\theta\approx-4/9\,\Delta\lambda\tan(\theta-\varphi)\cos^2(\theta-\varphi)/\sin^2\alpha_r\approx-4\Delta\lambda\,h^2/9\tan(\tfrac{1}{2}\varphi_d) \quad (23)$$

upon dropping the small drag correction in the factors, since the global optimum Δ's will prove next to be very small.....

Annually Optimal Small Hawt Blade

The net power at the design point is lowest for the smallest C_D/C_L ratio ε_o, which occurs at the best α_o. But any variation of the wind will perturb the independent variable θ and so the operating point $\varphi(\theta)$ away from the design . Then to maintain the optimum $\varphi_o(\theta)$ the design angle of attack should be the robust α_r found above. This section finds the best compromise α_d between c_p peak breadth in α_r and height in α_o for the highest mean power.

For a given θ the net c_p is stationary at the optimum $\varphi_o(\theta)$ (and $\varepsilon_{o)}$, and from (9) varies with φ as

$$c_p = c_{po}(\theta) - x(1+x^2)F\,(6\sin\varphi_o - 3\varepsilon_o\cos\varphi_o)(\varphi-\varphi_o)^2 \quad (24)$$

Where $(\varphi-\varphi_o)$ will be Taylor-expanded in terms of the $\delta\theta$ variation of θ from (23). This explicitly shows how the deviation of the power from the robust always-optimal varies as the square of not only $\delta\theta$ [1] but also the square of the deviation of the pitch from the robust value. If the pitch is robust, the next even order quartic $(\delta\theta)^4$ term must lead. If ε is simultaneously varied from ε_o add $(\varepsilon-\varepsilon_{o)}\{1+(\varphi-\varphi_o)\,d/d\varphi\}d\,c_p/d\varepsilon$ for the increase in the drag loss at constant θ or

$$x(1+x^2)\,F\{-\tfrac{1}{2}\sin\varphi_d\sin2\varphi_d + \sin(\varphi_d+\tfrac{1}{2}\varepsilon_{o)})(\varphi-\varphi_o)\}\,d^2\varepsilon/d\alpha^2(\alpha-\alpha_o)^2 \qquad (25)$$

For the NACA 23018 [6] e=.91 α_o =.175=10° ε_o=1/80=.7° and $b=d^2\varepsilon/d\alpha^2\approx$.45. This predicts a 61% higher ε= 1.13 at α=0°or 20° whereas ε is really infinite at α=0 and high at stalled 20° so its range is less than say ±5° without higher order terms. Of course the airfoil shape should be tuned along the wing to keep α_o as close to α_r as possible. The method here finds the best compromise of the outstanding difference. Now $\alpha-\alpha_o$ can be expanded as $\alpha_d-\alpha_o + \varphi-\varphi_d$ because the pitch λ is fixed.

Averaging (denoted by underlining) over the small variation of φ equally above and below φ_d, and again evaluating trigonometric factors at the design point and ignoring small drag terms, the extra c_p variation from always optimal $c_{po}(\theta)$ is approximately

$$x(1+x^2)\,F\,b\,\sin\varphi_d\,[-\tfrac{1}{2}\sin2\varphi_d\,\{(\alpha_d-\alpha_o)^2+\underline{(\varphi-\varphi_d)^2}\} + 2\,(\underline{\varphi-\varphi_o)\,(\varphi-\varphi_d)}\,(\alpha_d-\alpha_o)] \quad (26)$$

In the first expanding $\varphi-\varphi_d$ as $\varphi-\varphi_o + \varphi_o-\varphi_d$ and squaring generates a term in $(\varphi-\varphi_o)^2$ which is negligible vs the last term in (26) by $b\sin(2\varphi_d)/12$. In the second the $(\varphi-\varphi_o)^2$ term is smaller by $b(\alpha_d-\alpha_o)/3$ or at least .026 as $|\alpha_d-\alpha_o|$ is less than α_o. Both have a cross factor of $\varphi-\varphi_o$ by $2(\varphi_o-\varphi_d)= 4\,\delta\xi/3$. Thus the **$\alpha_d$ sensitive** part of the net of the means of (24) and (26) is

$x_d\,(1+x_d^2)F\sin\varphi_d$ times

$6(\underline{\varphi-\varphi_o)^2} + \tfrac{1}{2}b\sin2\varphi_d\,\{(\alpha_d-\alpha_o)^2+4(\underline{\varphi-\varphi_o)}\,\delta\theta/3\} - 8b\,(\underline{\varphi-\varphi_o)}\delta\theta/3\,(\alpha_d-\alpha_o)$ (27)

And using $\varphi-\varphi_o=\delta\theta\,d(\varphi-\varphi_o)/d\theta$ and (23), this sensitive factor is (28):

$6\{4(\underline{\alpha_d-\alpha_r)}\,\underline{\delta\theta\cot\tfrac{1}{2}\varphi h^2/9\}^2} + \tfrac{1}{2}b\sin2\varphi_d\{(\alpha_d-\alpha_o)^2+16(\alpha_d-\alpha_r)\cot\tfrac{1}{2}\varphi\,(\underline{\delta\theta}^2h^2/27\} - 32b(\alpha_d-\alpha_r)\,\cot\tfrac{1}{2}\varphi\,(\underline{\delta\theta)^2}\,(\alpha_d-\alpha_o)h^2/27$

Hence the optimum α_d satisfies the linear equation (29):

$32(\alpha_d-\alpha_r)[2h^4\cot^2\tfrac{1}{2}\varphi - bh^2\cot\tfrac{1}{2}\varphi]\,(\underline{\delta\theta)^2}/27 + (\alpha_d-\alpha_o)\,b\,[\sin2\varphi_d - 32\,h^2\cot\tfrac{1}{2}\varphi\,(\underline{\delta\theta)^2}/27] = -8b\,h^2\sin2\varphi_d\,\cot\tfrac{1}{2}\varphi\,(\underline{\delta\theta)^2}/27$

The last term in the first and second coefficients is at least .13 less than the first term in the first so the former is negligible and the latter confirms that for dominant $(\underline{\delta\theta)^2}$ variation α_d is much closer to α_r than to α_o.

As an example consider the temporal variation of X and so all the $x=\cot\underline{\theta}$ with windspeed V around V_d with near constant rotor $C_P=XC_T$. For rapid fluctuations, rotor inertia stops the rpm changing quickly. For a synchronous generator the grid frequency keeps the rpm constant so then X always varies as V^{-1}. For slow wind variations and an ideal cubic rpm load such as a fluid dynamic churn for mixing or heat, X is constant. For a permanent magnet generator connected to a dissipative load, the power consumed is proportional to rpm squared, so X varies a $V^{1/2}$. A positive displacement rotary pump against a fixed pressure head for unvarying load torque has $V^2\,C_T$ constant or X varying as V^2. So consider in general $x\propto V^g$, $g^2>0$ even for cubic loads. Then with $\tau=V/V_d$, $\delta\theta\approx\tfrac{1}{2}g\sin2\theta\;\delta\tau/\tau_d$.

Whilst still ignoring the variation of trigonometric factors with θ varying from θ_d, here the time average will effectively include the V^3 scaling of the power available by using , with $q(\tau)$ the frequency of winds between τ and $\tau+dt$, a power weighting $p(\tau)=\tau^3q(\tau)\,/\,\int\tau^3q(\tau)\,d\tau$. This peaks at the peak power spectrum design point $\tau=1$ $V=V_d$, as the area (net power) under the multiplication of the two (parabolic) peaked curves is maximum when the peaks coincide. (Their abscicas θ and V are close to globally matched in the prime synchronous and wind shear cases of constant Ω where at large x, $\theta\propto V$.)

For the fairly tight Rayleigh distribution $q(\tau)=4\tau\exp(-2\tau^2)$ with mean V of .627 V_d and a mean power density of .47 of $\tfrac{1}{2}\rho V_d^3$, matching the peak and its second derivative at V_d gives a consistent and under approximation of quadratic about the peak $p(\tau)=3\{1-4(\tau-1)^2\}/2$ between zeroes at $\tau=.5$ and 1.5. Then the $(\delta\tau)^2p(\tau)$ terms integrate to 1/20 so dividing by $(\tfrac{1}{2}g\sin2\theta)^2$ and multiplying by 270/4

$(\alpha_d-\alpha_r)8\,h^4\cot^2\tfrac{1}{2}\varphi_d + (\alpha_d-\alpha_o)\,b\,[270\sin2\varphi_d/g^2\sin^23\varphi_d - 4h^2\cot\tfrac{1}{2}\varphi_d] \approx -b\,h^2\sin2\varphi_d\,\cot\tfrac{1}{2}\varphi_d$ (30)

Fig 2 presents g^2=1 calculations for the NACA23018 lift to drag data above. The optimal local coefficient of performance $c_P(x)$ was calculated from (8) and then numerically integrated to get the rotor coefficient $C_{Po}=\int c_{Pm}\,dx^2 \;/\; X^2$ which peaks when $C_{Po}=c_{Po}$. The intersection of these curves helps to locate the peak C_{Po} at X=5 θ=11.3 deg as its maximum is very broad. To give this effective tip speed ratio, the actual tip speed ratio must be increased relatively by .221 $2\pi \sin\varphi/B$ or for the standard B=3, by 1.062 to 5.31.

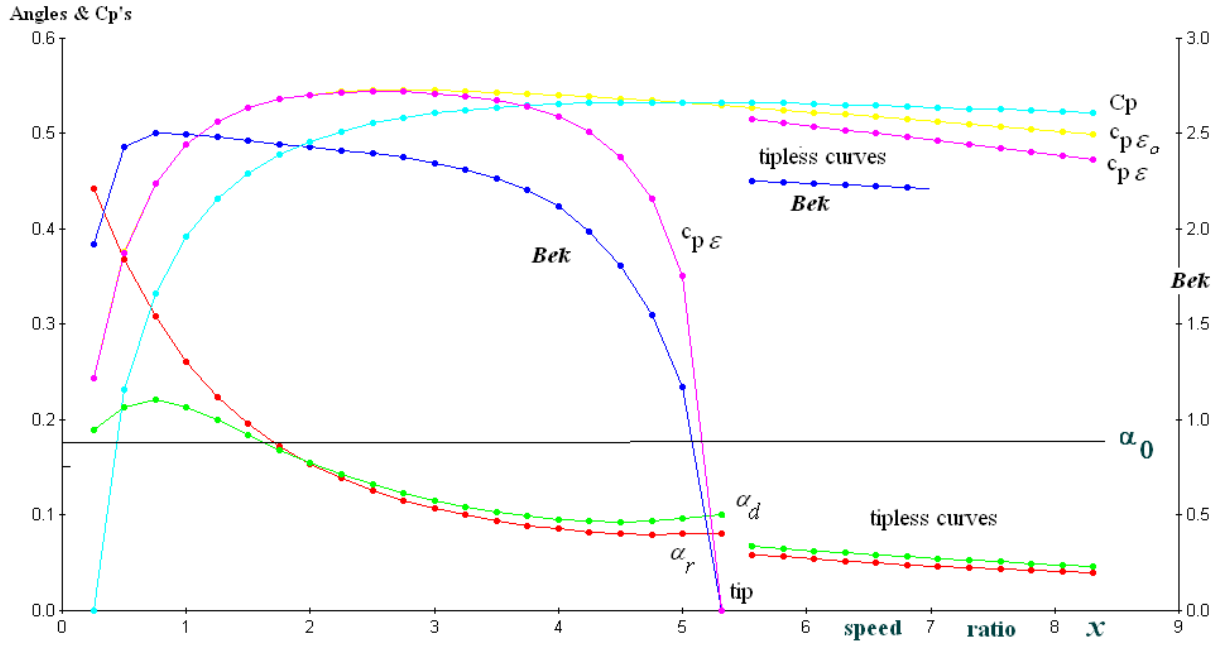

Figure 2 Optimum Hawt blade design chord and angle of attack

The constant term in equation (32) affects the results by less than 3%, so ignoring that, the best α_d is indeed a weighted average of α_r and α_o as anticipated in the introduction. Iterating in α_r (16) and (18) to correct for its ε being greater than ε_o and for its $d\varepsilon/d\alpha$ had no noticeable effect . Actually α_d does not exceed the stall value due to the moderating influence of the relatively small α_o at small x. The leading coefficients are equal at about φ=30° or x=1, so the robust α_r increasingly dominates the minimum drag α_o moving out in the robust zone. Conversely the sum of the two quadratic losses from the ideal highest and always optimal is in turn dominated the reduction of the peak height by non-minimal drag/lift shown as $c_{p\varepsilon}$ versus $c_{p\varepsilon o}$

The lines above the tip X show the design angle of attack and chord with no tip. The best angle of attack then follows above the robust at a proportion $(\alpha_d-\alpha_r)\,/\alpha_r$ rising to $3.7b\alpha_o/\,g^2$ or 29% above. The design net chord *Bek*

slowly declines because of the rise both in this proportion and in the drag correction factor in the robust chord, agreeing with Stewart[2]. Without these drag effects the design=robust *Bek* rose to an asymptote of 8/3 and of course c_p and *C*p rise to an asymptote of 16/27=.593. [1]

The lines just below the tip *X* show the Prandtl *F* influence in raising the robust angle of attack and the design proportion above it due to the local weakening of the robust dominance with h^4, so much so that the design angle reaches a minimum of .096 or 5.5° at about x=4.5 . Synchronously at g=-1 these help to relieve the high wind tip bending moment by reducing its design stall margin.

Really $(\underline{\delta\theta})^2$ and $(\underline{\delta\tau})^2$ could be generalised as variances about the design point. To do so for the open-ended Rayleigh distribution brings in too much variation far from the peak and raises the above close-to-peak value of .05 by an inappropriate amount to .118. But statistical formulae are suitable for the tighter fixed end distribution generated by the blade element sweeping through windshear.

Thus if the wind shears linearly as $V_0(1+ m\sin\phi)$ where $m= kx/X$ to be $V_0(1+ k)$ at the tip's highest point azimuth $\phi=\pi/2$, the cubic power weighting is $p(\phi)= (1+ m\sin\phi)^3/a$ where the integration will be averaging over ϕ so then $a=1+3m^2/2$. Then the variation $\delta\tau_0=m\sin\phi$ in $\tau_0= V/V_0$ has power weighted averages $a\underline{\delta\tau_0}=3m^2/2+3m^4/8$ and $a(\underline{\delta\tau_0})^2 = ½\, m^2+9m^4/8$. The power mean $\underline{\tau}_0$ of $1+\underline{\delta\tau_0} \approx 1+3m^2/2-15m^4/8$ and the true minimum variance about it is

$(\underline{\delta\tau_0})^2 - \{\underline{\delta\tau_0}\}^2 \approx ½\, m^2-15m^4/8$, so finally taking the design as this power mean, $\{\underline{\delta\tau}\}^2 \approx ½\, m^2-27m^4/8$; or at k=1/3 when the top wind is twice the bottom and at representative x/X=.7, about .017 versus .05 Rayleigh; so the robust would then be about one third as dominant for an ideal cubic load as calculated above. Calculated exactly for the tip, $\{\underline{\delta\tau}\}^2$ is .029 . When g >0 this independent variance must be added to the Rayleigh-derived one, and its increase towards the tip helps to make the robust more dominant and more uniformly so.

Every other independent source of variation likewise adds further to the dominance of the robust blade setting. The principal unaccounted (hard to quantify) variation is in the wind direction, potentially very significant for big Hawts with their active yaw power consumption (but in yaw the trisection has only been proved in the limit of high x [1]) At the azimuths, the yaw adds to x. At all positions x is factored by the yaw^2, so the θ variance would have terms in yaw^2 and yaw^4, which would need to be calculated from wind data and the Hawt yaw response.

Conclusion

The drag and tip-corrected Blade Element Momentum theory that is the basis of most Hawt computer design has been analytically optimised for maximum annual power. These refinements do not substantially affect the optimum apparent wind angle φ being 2/3 of the nominal θ. But the design angle of attack to robustly maintain the optimum as the wind varies is substantially increased above the naive ⅓ θ in the tip region because the tip loss (1-*F*) increases with windspeed at fixed rpm.

The section should be chosen with the minimum drag to lift ratio at the robust angle of attack. This favours increasingly thin sections on the outer blade. If the angle of attack for its best drag to lift is different from the robust, a linear equation gives the compromise design angle of attack with the best mean annual power in terms of the wind and load regimes. The typical domination of the robust angle outside the blade root is moderated by the tip correction, again raising the design angle of attack in the tip zone, which along with the optimal thin sections helps its stall-regulation of bending moment.

12. Wilson, R.E.& Lissaman, P.B.S *Applied Aerodynamics of Wind Power Machines,* Oregon State Univ Corvallis, 1974 http://ir.library.oregonstate.edu/dspace/handle/1957/8140

12. Steffen Wußow *et al* 2007 "3D-simulation of the turbulent wake behind a wind turbine" *J. Phys.: Conf. Ser.* 75 012033 (8pp) http://www.iop.org/EJ/abstract/1742-6596/75/1/012033

13.Mikkelsen R. "Actuator disk methods applied to wind turbines" *PhD Thesis*, Technical University of Denmark, Lyngby, 2003.

14. Farthing, S. P. "Robustly Optimal Fixed Pitch Hawt with Tip Correction and Drag". *AIAA J.* Vol 46 #6 2008 p 1549-1553

Coleman RP, Feingold AM, Stempin CW. Evaluation of the induced-velocity field of an idealized helicopter rotor. *Technical Report NACA-WR-L-126*, 1945.